AFRL-RY-WP-TR-2012-0094

DEVELOPMENT OF CHIP-BASED FREQUENCY COMBS FOR SPECTRAL AND TIMING APPLICATIONS

Yoshi Okawachi

Cornell University

DECEMBER 2011
Final Report

Approved for public release; distribution unlimited.

See additional restrictions described on inside pages

STINFO COPY

AIR FORCE RESEARCH LABORATORY
SENSORS DIRECTORATE
WRIGHT-PATTERSON AIR FORCE BASE, OH 45433-7320
AIR FORCE MATERIEL COMMAND
UNITED STATES AIR FORCE

NOTICE AND SIGNATURE PAGE

AFRL-RY-WP-TR-2012-0094 HAS BEEN REVIEWED AND IS APPROVED FOR PUBLICATION IN ACCORDANCE WITH THE ASSIGNED DISTRIBUTION STATEMENT.

*//Signature//

BRYCE E. SCHUMM
Project Manager
LADAR Technology Branch
Multispectral Sensing and Detection Division

//Signature//

BRIAN D. EWERT, Chief
LADAR Technology Branch
Multispectral Sensing and Detection Division

//Signature//

TRACY W. JOHNSTON, Chief
Multispectral Sensing and Detection Division
Sensors Directorate

*Disseminated copies will show "//signature//" stamped or typed above the signature blocks.

REPORT DOCUMENTATION PAGE	*Form Approved OMB No. 0704-0188*

1. REPORT DATE *(DD-MM-YY)*	2. REPORT TYPE	3. DATES COVERED *(From - To)*
December 2011	Final	27 July 2010 – 31 October 2011

4. TITLE AND SUBTITLE
DEVELOPMENT OF CHIP-BASED FREQUENCY COMBS FOR SPECTRAL AND TIMING APPLICATIONS

5a. CONTRACT NUMBER
FA8650-10-1-7064

5b. GRANT NUMBER

5c. PROGRAM ELEMENT NUMBER
62702E

6. AUTHOR(S)
Yoshi Okawachi

5d. PROJECT NUMBER
DARPA

5e. TASK NUMBER
YJ

5f. WORK UNIT NUMBER
ARPRYJ0Q

7. PERFORMING ORGANIZATION NAME(S) AND ADDRESS(ES)
Cornell University
373 Pine Tree Road
Ithaca, NY 14850-2820

8. PERFORMING ORGANIZATION REPORT NUMBER

9. SPONSORING/MONITORING AGENCY NAME(S) AND ADDRESS(ES)
Air Force Research Laboratory
Sensors Directorate
Wright-Patterson Air Force Base, OH 45433-7320
Air Force Materiel Command
United States Air Force

10. SPONSORING/MONITORING AGENCY ACRONYM(S)
AFRL/RYMM

11. SPONSORING/MONITORING AGENCY REPORT NUMBER(S)
AFRL-RY-WP-TR-2012-0094

12. DISTRIBUTION/AVAILABILITY STATEMENT
Approved for public release; distribution unlimited.

13. SUPPLEMENTARY NOTES
DARPA PAO Case Number: 19079, cleared 26 March 2012. Report contains color.

14. ABSTRACT
This report describes research results in developing the technology for the generation of a broadband parametric frequency combs with flexible operating wavelengths and comb spacing. The research showed the flexibility in operating wavelengths with demonstration of comb generation with a 1-mm pump. Technology was further developed at 1.5 mm and showed that with appropriate waveguide engineering, the comb can span an octave of bandwidth, which is crucial for self-stabilization. Additionally, through modification of the resonator design, results showed the ability to generate combs with various spacing ranging from 200 GHz to 20 GHz. Finally, combs were utilized to generate a high-repetition-rate, ultrafast pulse source.

15. SUBJECT TERMS
frequency comb, femtosecond laser

16. SECURITY CLASSIFICATION OF: a. REPORT	b. ABSTRACT	c. THIS PAGE	17. LIMITATION OF ABSTRACT:	18. NUMBER OF PAGES	19a. NAME OF RESPONSIBLE PERSON (Monitor)
Unclassified	Unclassified	Unclassified	SAR	28	Bryce E. Schumm **19b. TELEPHONE NUMBER** *(Include Area Code)* N/A

Standard Form 298 (Rev. 8-98)
Prescribed by ANSI Std. Z39-18

Table of Contents

List of Figures

Figure **Page**

1. Executive Summary

We have investigated the generation of broadband frequency combs via parametric mixing in CMOS-compatible silicon nitride microresonators. In this system amplification via the nonlinear process of four-wave mixing (FWM) leads to amplification of frequency components at microresonator sidemodes of the pump. At sufficiently high powers the threshold for parametric oscillation occurs, and the process can continue to cascade to other sidemodes as the power is increased.

This report describes our results to develop the technology for the generation of a broadband parametric frequency comb with flexible operating wavelength and comb spacing. We showed the flexibility in operating wavelength with our demonstration of comb generation with a 1-μm pump. We further developed our technology at 1.5 mm and showed that with appropriate waveguide engineering, the comb can span an octave of bandwidth, which is crucial for self-stabilization. Additionally, through modification of the resonator design, we have shown the ability to generate combs with various spacing ranging from 200 GHz to 20 GHz. Finally, we have utilized the comb to generate a high-repetition-rate, ultrafast pulse source.

In conclusion, we have shown that the silicon nitride resonators offer potential as a platform for robust, integrated, chip-scale comb source. The system can be further improved to develop stabilized comb sources that can be utilized for various spectroscopic applications and the creating of highly robust and compact all-optical clocks.

2. Introduction

Over the past decade a revolution has occurred in techniques for producing optical frequency combs [1]. Such combs can provide a high precision frequency "ruler" for performing spectroscopic measurements in the infrared (IR), visible, and ultraviolet regimes [2] and can be applied to broad-band laser-based gas sensing [3] and molecular fingerprinting [4]. For the case in which the combs span more than an octave of the central frequency, such combs can be used to create an optical clock.

Generation and stabilization of optical frequency combs have traditionally relied on modelocked solid-state and fiber lasers, which are capable of producing ultrashort pulse trains in the visible and near-IR range. In numerous optical frequency comb demonstrations, a broadband, octave-spanning spectrum is often desired to be able to use a self-referencing technique for stabilization of the carrier-envelope-offset frequency f_{CEO}, which represents one of the two degrees of freedom for controlling the frequency comb from ultrafast solid-state lasers [5-7]. The self-referencing technique requires that the low-frequency portion of the spectrum be frequency-doubled and heterodyned with the high-frequency portion to produce a baseband beat note equal to f_{CEO}, which can be phase-locked to a microwave frequency standard [8]. This necessitates either direct generation of the octave-wide spectrum from the ultrafast source [9] or external spectral broadening mechanisms such as supercontinuum generation in microstructured fibers [9,10]. The other degree of freedom in frequency combs is the spacing between adjacent lines, which is determined by the cavity repetition rate f_R of the ultrafast laser. Precise stabilization of f_R can be achieved by locking a comb line to an atomic transition whereby f_R is determined by the precision of the locks divided by the line number ~ 10^6. Stabilization can also be achieved by photodetection of the periodic output pulse train and phase-locking a filtered high harmonic to a frequency standard or synthesizer. Complete control and stabilization of these two degrees of freedom has been demonstrated successfully with various solid-state and fiber laser platforms. The wavelengths of the optical frequency combs cover the visible and near-IR range due to availability of gain materials which are further expanded via supercontinuum generation in microstructured fibers.

Recently, cascaded optical parametric oscillation (OPO) in high-*Q* microresonators has been shown as a promising alternative approach for frequency comb generation [11-18]. Various cavity geometries such as suspended microtoroid or microsphere resonators have been shown to provide extremely high cavity quality factors *Q* reaching 10^9 for visible and infrared wavelengths [19]. In these implementations, the whispering gallery modes of the high-*Q* microresonators can be accessed externally with either a tapered fiber or prism, and the parametric interaction can be driven with a resonant continuous-wave (cw) pump. Experimental demonstrations of frequency combs using high-*Q* microresonators have commonly utilized exploited the $\chi^{(3)}$ nonlinearity of the constituent material such as silica [12,13,15,18]and calcium fluoride [14]. A practical drawback to high-*Q* resonator designs utilizing whispering gallery modes that the coupling efficiency and the threshold power for parametric oscillation with the tapered fiber access are extremely sensitive to fiber displacement from the cavity and maintaining the *Q* of these cavities is known to require a nitrogen-purged environment to avoid absorption from ambient water vapor.

In our research, we utilize silicon nitride microresonators for parametric frequency comb generation [20,21]. Unlike many other high-*Q* resonator designs, the resonator and the coupling waveguide are monolithically integrated. Thus, the entire on-chip configuration of CMOS-compatible microresonators can provide robust operation in ambient conditions yielding a truly monolithic, robust, and highly compact frequency comb source capable of tight integration with control electronics and other photonic components such filters and modulators.

3. Parametric Frequency Comb Generation

Frequency comb generation in microresonators is dependent on the parametric four-wave mixing (FWM) which is dependent on the $\chi^{(3)}$ nonlinearity. In this system, parametric amplification via the FWM leads to amplification of frequency components at microresonator sidemodes of the pump. At sufficiently high powers, the FWM gain leads to parametric oscillation. As the power in the sidemodes build up, they become pumps for cascaded FWM. Furthermore, higher order degenerate and non-degenerate FWM processes fill in all of the adjacent resonator modes, generating multiple new frequencies from a single-frequency input (Figure 1).

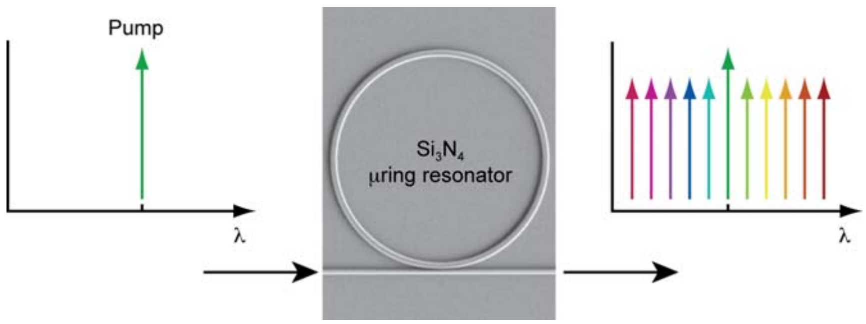

Figure 1. Schematic of an integrated silicon nitride ring resonator frequency comb generator with a scanning electron micrograph of a silicon nitride ring.

Engineering the dispersion of microresonators is essential for efficient generation of the cascaded OPO spectrum beyond an octave. With the typical cross-section of the microresonators ranging around optical wavelengths, the waveguide dispersion dominates over material dispersion, providing an essential design tool for broadband dispersion engineering [22-24]. For example, the normal dispersion introduced by the material can be compensated by the waveguide dispersion designed to be anomalous, so that the total chromatic dispersion can be kept near zero or slightly anomalous depending on the waveguide width for a given height. This condition provides the necessary phase-matching for cascaded parametric interactions within the microresonator. For silicon nitride waveguide, due to the high index contrast between the nitride core and oxide cladding, high mode confinement can be achieved in the structure, resulting in a large contribution from the waveguide dispersion (Figure 2). This allows for dispersion tailoring through engineering the waveguide cross-section size and shape. Unlike whispering gallery mode resonators, in most cases, phase-matching is achieved independent of cavity length which allows a larger degree of freedom in the choice of the generated comb spacing and operating wavelength. Broadband comb generation requires operation anomalous dispersion regime of the resonator to satisfy phase-matching conditions. Dispersion simulations using a finite-element mode solver indicate that a broadband anomalous dispersion regime spanning nearly an octave is possible with appropriate waveguide cross-section engineering (Figure 2) [25].

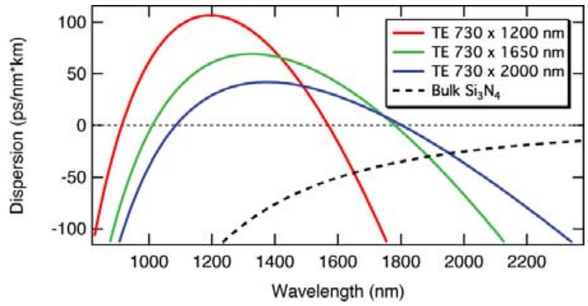

Figure 2. Simulated dispersion for silicon nitride waveguides.

4. Frequency Comb Generation with a 1-μm Pump

For frequency comb generation with a 1-μm pump, we engineer the resonator dispersion such that the total dispersion is anomalous over a broad bandwidth surrounding the pump wavelength. In our experiment, we amplify a tunable single-frequency laser centered at 1064 nm with a ytterbium-doped fiber amplifier (YDFA) and inject it into a nanowaveguide which is coupled to the microring resonator (Figure 3). Both the coupling waveguide and the microring were fabricated in a silicon nitride layer which is deposited on a silicon dioxide substrate using low pressure chemical vapor deposition. We designed our devices for a core thickness of 600 nm. To mitigate variations in fabrications of film thickness, waveguide width and waveguide etch angles, we fabricated multiple chips with nominal waveguide widths varying from 800 nm to 1200 nm in 50-nm increments. For each width, ring resonators of three different diameters, 100, 200 and 400 μm are made. For each radius coupling gaps are varied across 12 waveguides from 150 to 425 nm between the ring and waveguide.

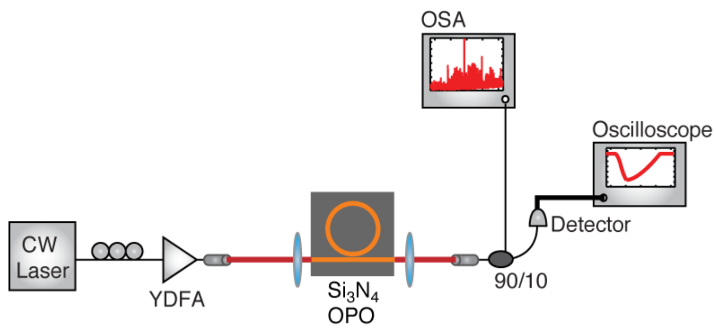

Figure 3. Schematic of experimental setup for frequency comb generation.

Examples of spectra generated from the microresonator are shown in Figure 4 for various detunings from the cavity resonance. The resonator measures 1150 nm in width, which yields anomalous dispersion at the pump wavelength of 1064 nm, which is a necessary condition for producing parametric amplification. The microring has a 200-μm diameter and the coupling gap is 375 nm between ring and waveguide. The pump power coupled to the waveguide is 250 mW. The pump wavelength is tuned into a cavity resonance, such that a stable "thermal lock" is achieved [26]. The circulating power in the microring builds up and leads to parametric oscillation [Figure 4(a)]. As the power increases, cascaded FWM occurs, leading to the generation of multiple oscillating modes. The density of comb lines increases as the pump frequency is tuned deep into the cavity resonance [Figure 4(b)], and adjacent cavity modes separated by 230 GHz are excited via multiple FWM processes [Figure 4(c)]. The comb lines are generated over a wavelength span of 406 nm, corresponding to a 97.3 THz frequency span [27].

While the previous parametric comb generation demonstrates a broad bandwidth, as shown in Figure 4(c), not all of the comb lines have filled in. We attribute this to linear losses in both the microresonator and coupling nanowaveguide along a low coupling quality factor between the waveguide and cavity. The coupling separation between the nanowaveguide and the microresonators were not optimal in the early designs. The coupling coefficient must be carefully matched to the ring losses to achieve the critical coupling condition at which all the power from the waveguide is dropped into the resonator. When redesigning the devices we increased the thickness of the core nitride film. This enables a broader range of widths that give anomalous group-velocity dispersion (GVD) for both TE and TM polarizations.

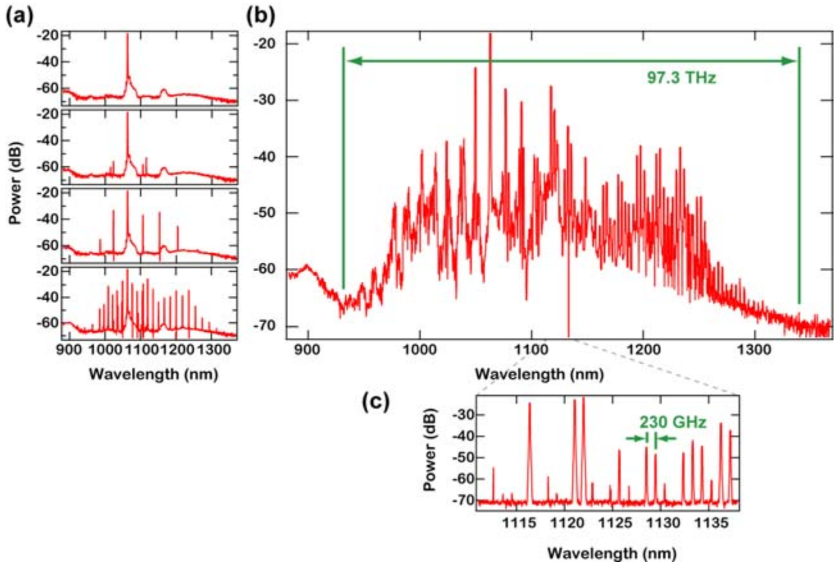

Figure 4. (a) Frequency comb generation in microring resonator as pump wavelength is tuned into cavity resonance. (b) Frequency comb with 97.3 TH bandwidth. (c) Comb with line spacing of 230 GHz.

For the next generation of devices, we fabricated the same range of widths but focused only on the 100-µm radius rings, which were the most promising for broadband comb generation. On each chip in this generation we fabricated 25 rings with coupling gaps varying from 200 nm to 825 nm. The wide range of coupling gaps ensures that even with improved quality factors we will be able to pump near critical coupling in at least one of the devices. Additionally, we reduced the physical chip size to only 2 mm by 10 mm. The smaller size aims to diminish the effects of potential stitching-induced losses from the e-beam lithography.

Silicon nitride ring resonators with a cross section of 725 nm by 1000 nm and a 100-µm radius are fabricated. The most recent chips we fabricated have now greatly improved coupling efficiencies, in the TM polarization, which allow us to significantly increase the amount of power in the microresonators. The generated comb spectra are shown in Figure 5(a). While the bandwidth is reduced to 55.5 THz, the oscillation threshold is reduced to <80 mW and, as seen in Figure 5(b), every adjacent comb line separated by the free-spectral range of the resonator is filled in. The comb line spacing is 230 GHz.

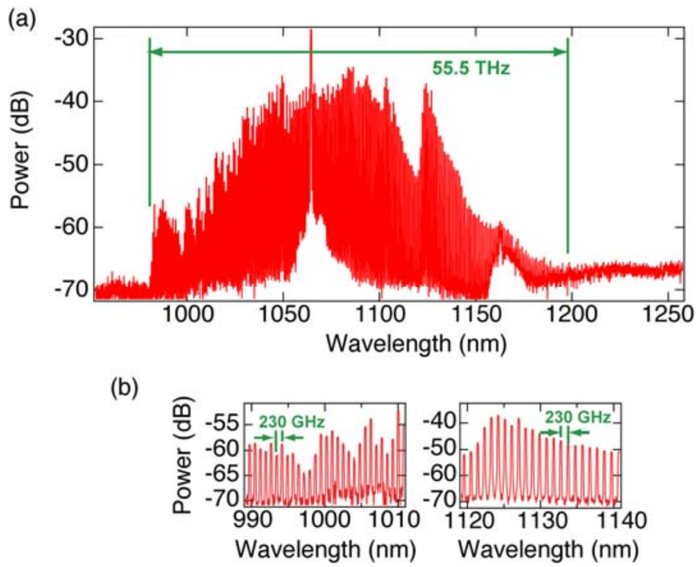

Figure 5. (a) Frequency comb with 55.5 THz bandwidth. (b) Comb with line spacing of 230 GHz.

5. Octave-Spanning Frequency Comb

We have investigated the generation of octave-spanning frequency combs via parametric mixing in CMOS-compatible silicon-nitride microring resonators using a single-frequency pump laser at 1.5-µm pump. Frequency combs spanning an octave enable full stabilization of the comb through a well-established *f*-2*f* self-referencing technique. In order to achieve broadband comb generation, the resonator dispersion must be engineered to have a broad region of anomalous dispersion. Numerical simulations indicates that large anomalous dispersion regions spanning nearly an octave are possible with appropriate cross-section engineering.

In our current experiments, we amplify a tunable single-frequency laser centered at 1562 nm with an erbium-doped fiber amplifier and inject it into a nanowaveguide, which is coupled to the microring resonator. The input polarization is adjusted to quasi-TE using a fiber polarization controller. The nanowaveguide acts as the coupling waveguide for the microring resonator. Both the coupling waveguide and the microring have cross-sections of 725 nm by 1650 nm with a 10° sidewall angle, and the microring has a 200-µm diameter. The loaded Q is approximately 10^5. The power inside the coupling waveguide is 400 mW when the pump wavelength is detuned from a cavity resonance for an amplifier power of 2 W. The output is collected using an aspheric lens and sent to an optical spectrum analyzer (OSA).

A typical frequency comb spectrum is shown in Figure 6. The pump power in the coupling waveguide when detuned from a cavity resonance is 400 mW for an amplifier power of 2 W. As the pump frequency is tuned into a cavity resonance, the circulating power in the microring builds up beyond threshold for parametric oscillation. As the circulating power is further increased, cascaded FWM occurs, leading to the generation of comb lines. Higher-order degenerate and non-degenerate FWM processes fill in adjacent comb lines, increasing the overall comb density. The comb lines are generated over a wavelength span of 1180 nm, ranging from 1170 nm to 2350 nm, corresponding to 128 THz and over an octave of bandwidth [25]. The comb spacing, or free spectral range (FSR), is 226 GHz. We investigate the tuning performance of the frequency comb with pump power and show that the position of the comb lines can be shifted by 29 GHz. We estimate that the comb spacing can be tuned by 36 MHz over this range.

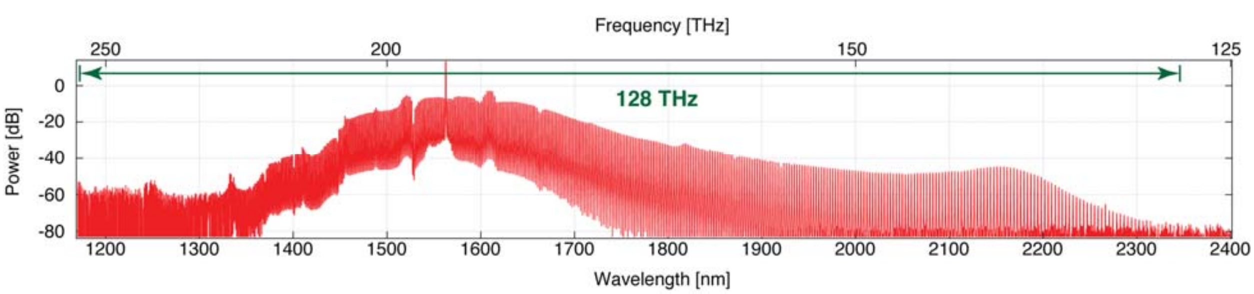

Figure 6. Octave-spanning frequency comb generation with a 1.5-µm pump.

Additionally, we characterize the RF amplitude noise of the system (Figure 7). We filter a 9-nm segment of the frequency comb spectrum and send it to a fast photodiode detector, and the electrical signal is characterized using an RF spectrum analyzer. As the pump wavelength is tuned into a cavity resonance, we observe a 30-dB reduction in the RF amplitude noise [25]. This low-noise state is maintained as the pump wavelength is further tuned into the resonance. We believe this is a result of the comb transitioning into a phase-locked state where the comb lines have a fixed relationship between them.

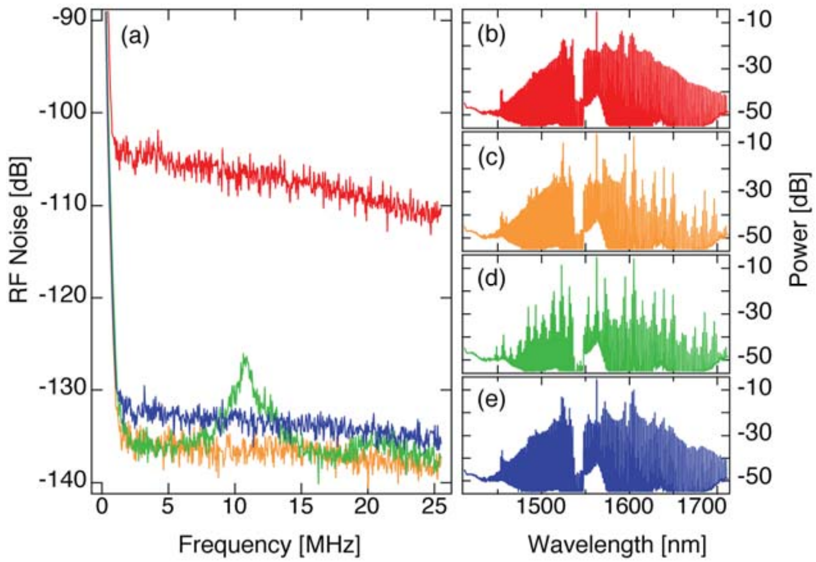

Figure 7. RF characterization of parametric comb. (a) RF noise spectra of parametric frequency comb. A 9-nm portion of the optical spec- trum is filtered from the comb for RF measurement. The noise is measured at four different pump detunings over a 10-GHz range as the pump is tuned into the cavity resonance. (b)-(e) show the corresponding optical spectra after the 9-nm section is filtered.

6. Low-Repetition-Rate Comb Generation

We investigate frequency comb generation with lower FSR silicon nitride resonators. In order to enable a direct link between microwave frequencies and optical frequencies, the FSR of the comb must be within the detection range of a fast photodiode (10's of GHz). Simulations of the group index allow us to calculate the path length required for each FSR. To achieve FSRs of 80, 40, and 20 GHz, the path length of the resonators must be increased to 1.8, 3.6, and 7.2 mm, respectively. These increased path lengths will no longer fit on a single e-beam field using the simple ring geometry employed in all previous parametric comb generation. In order to maintain low losses, the resonator must be written within a single e-beam field to avoid stitching errors at the boundaries. Therefore, to accommodate the increased path lengths, we fabricate a specific spiral geometry for each resonator as shown in Figure 8. The spiral design allows us to maintain a small footprint and employ a constant semi-circular coupling region to enable critical coupling between the bus waveguide and the resonator independent of path length. Bends in the resonators have radii greater than 100 μm to ensure that dispersion introduced by the bends is negligible as compared to the dispersion in the straight sections critical for proper operation of the frequency comb. Because of the relatively large resonator sizes required for such an FSR, we modify the resonator shape from a ring to an arbitrary enclosed spiral [Figure 8 (a)-(c)]. Figure 8(d)-(f) show the transmission spectra for the 20-, 40-, and 80-GHz FSR rings. The cross section is fixed for all of the spiral resonators and is 725 nm by 1650 nm.

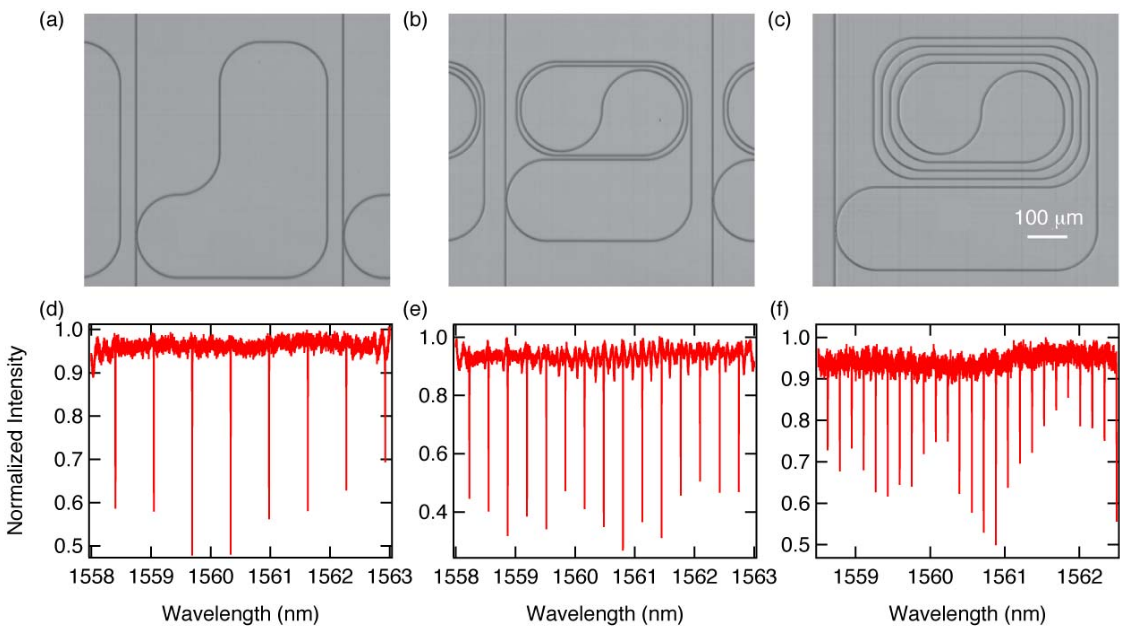

Figure 8. Micrographs of the (a) 80-, (b) 40-, and (c) 20-GHz FSR resonators and the corresponding transmission spectral for (d), (e), and (f), respectively.

The experimental setup for the low FSR comb is identical to that of the octave comb discussed earlier. The pump wavelength is tuned to a cavity resonance near 1562 nm. Input coupling losses to the coupling waveguide when off-resonance range from -7 to -9 dB. Figure 9 shows experimentally measured spectra for comb generation in three spiral resonators, with an FSR of

80, 40, and 20 GHz [28]. The 40- and 80-GHz combs require 2.1 W, and the 20-GHz requires 2.2 W to fill the entire comb spans which are 300 nm for the former two and 200 nm for the latter. Similar to [25], we observe that the amplitude noise of the combs, characterized with an RF spectrum analyzer, shows a reduction in the noise level during comb generation, which we believe is due to the system reaching a phase-locked state. The modulations in the 20-GHz comb spectrum result from the fact that, while it is sufficient for reaching the low noise state, the coupled power is insufficient for equalization of the comb lines. Each inset in Figure 9 shows a high resolution view of the respective comb in the low-noise state.

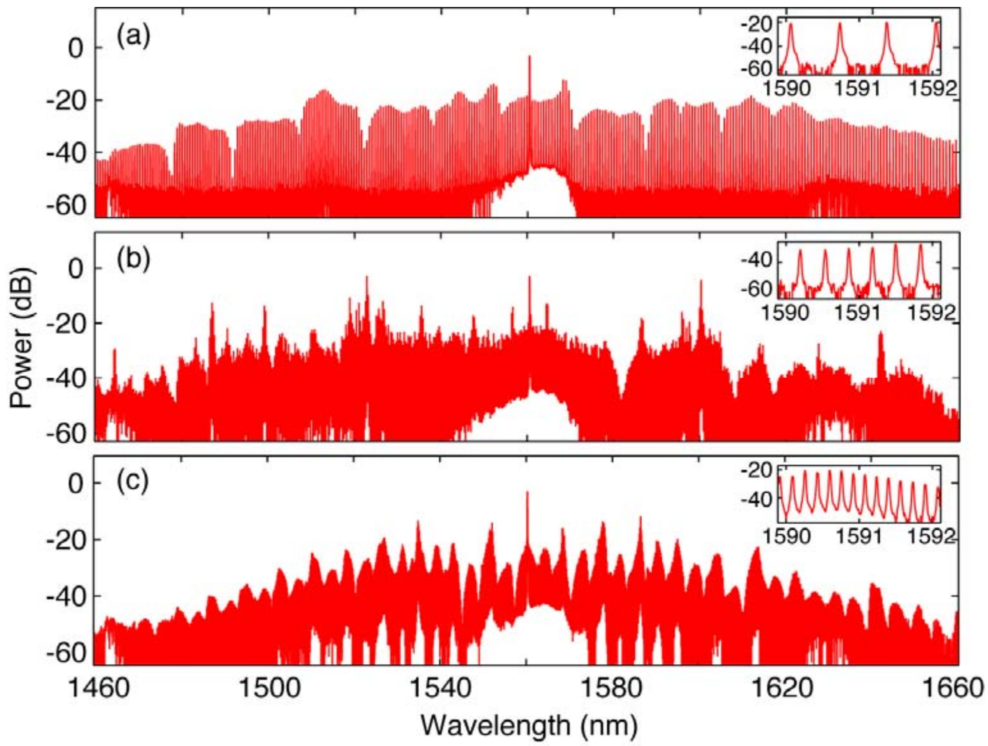

Figure 9. Frequency spectra generated from microresonators with FSR's of (a) 80 GHz, (b) 40 GHz, and (c) 20 GHz. A 2-nm section of each comb is inset in each figure to illustrate the spacing of the comb lines.

We characterize in more detail the spacing of the 20-GHz comb by measuring the RF beat note. A 1-nm section of the comb spectrum is filtered at 1540 nm and amplified with an EDFA. The output is sent to a fast photodiode detector and measured with an RF spectrum analyzer. Figure 10(a) shows the detected RF beat note (red line) and background noise measurement (blue line), which shows the detector response. The RF beat note has a frequency of 19.83 GHz with a full width at half maximum (FWHM) of 3.6 MHz, which is significantly narrower than previous observations [29]. Additionally, we perform a beat note measurement with a 30-nm section of the comb [Figure 10(b)]. The linewidth of the beat note, shown in Figure 10(c), remains unchanged with the 30× increase in the filtered spectral width, thereby confirming that our measured linewidth is not due to variations in comb spacing. We have observed previously that pump power fluctuations lead to thermal changes in the resonator that shift both the resonance and FSR [25]. We believe that our measured linewidth is limited primarily by the amplitude noise from the EDFA and the laser. We estimate a frequency shift of approximately 100 kHz/mW with respect to coupled power in the bus waveguide.

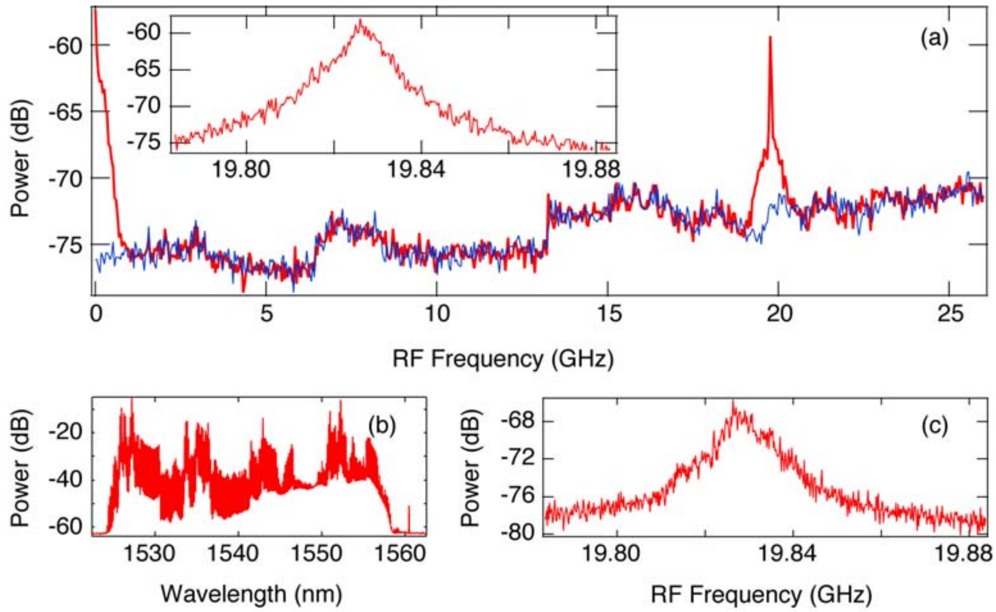

Figure 10. RF characterization of 20-GHz comb. (a) Measured RF frequency spectrum for the 20-GHz comb with a peak at 19.83 GHz (red trace) and background measurement (blue trace). (b) Filtered 30-nm segment of the 20-GHz comb. (c) RF frequency spectrum for 30-nm segment.

7. High-Repetition-Rate Ultrafast Pulse Source

We investigate the temporal characteristics of the parametric frequency comb. A mode-locked laser source produces a periodic train of ultrafast pulses at a rate given by the comb spacing. We expect that if the comb lines of silicon-nitride resonators have a definite phase relationship, then its output should consist of a periodic ultrafast waveform in the time domain. In our experiment, we filter a 25-nm section (32 comb lines) of a 100-GHz FSR parametric comb [Figure 11(a)], amplify and send it into an autocorrelation for temporal characterization. Figure 11(b) shows the normalized autocorrelation trace of the observed pulse train. The pulses have a repetition rate of 98.8 GHz, which corresponds to 10.1 ps, as is expected from the FSR of the comb. The full-width at half-maximum is 193 ± 5 fs [30], which we believe is limited by third-order dispersion. The peak power of the pulses is 1.2 W. The temporal output is stable as long as the pump is on resonance and there is no variation in coupling to the resonator. These results confirm our previous observation that the frequency comb transitions to a phase-locked state [25].

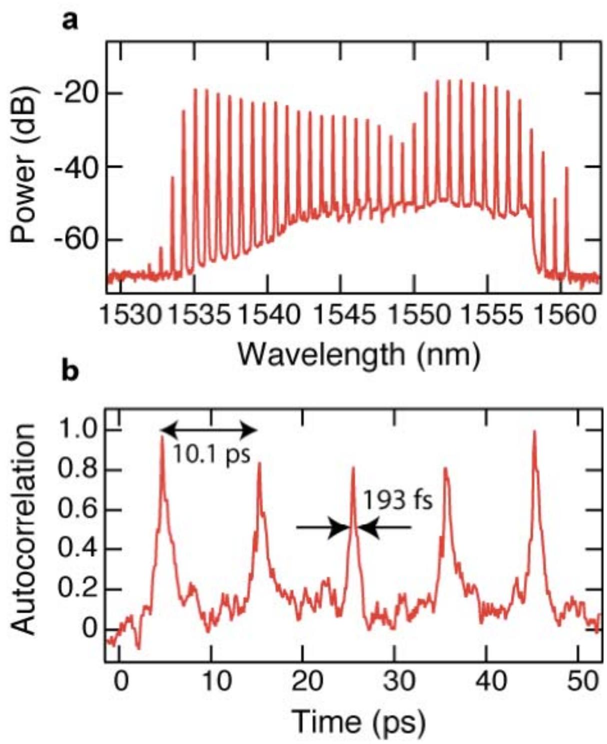

Figure 11. (a) Filtered optical spectrum of frequency comb with 99-GHz FSR. (b) Normalized autocorrelation trace of pulse train.

As described earlier, the silicon-nitride high-*Q* resonator platform allows for unmatched flexibility in terms of controlling the comb spacing, which is dictated by the resonator circumference, without changing the cavity dispersion. This provides the scope for designing and building a high-repetition rate pulse source with a desired pulse repetition rate. As a proof of principle demonstration, we use a 112-µm-radius ring-resonator, which corresponds to a free-spectral range of 225 GHz, for comb generation and pulse characterization. After filtering out a 25-nm section of the comb (14 lines) centered at 1543 nm [Figure 12(a)], and amplifying, we measure the pulses with the autocorrelator as before. As shown in Figure 12(b), we observe sub-

350 fs pulses at intervals of 4.44 ps, which correspond to 225 GHz repetition rate. Unlike other pulse sources, (such as a Ti:Sapphire laser) phase-locking takes place naturally in this system and there is no need for the presence of an additional saturable absorber [30].

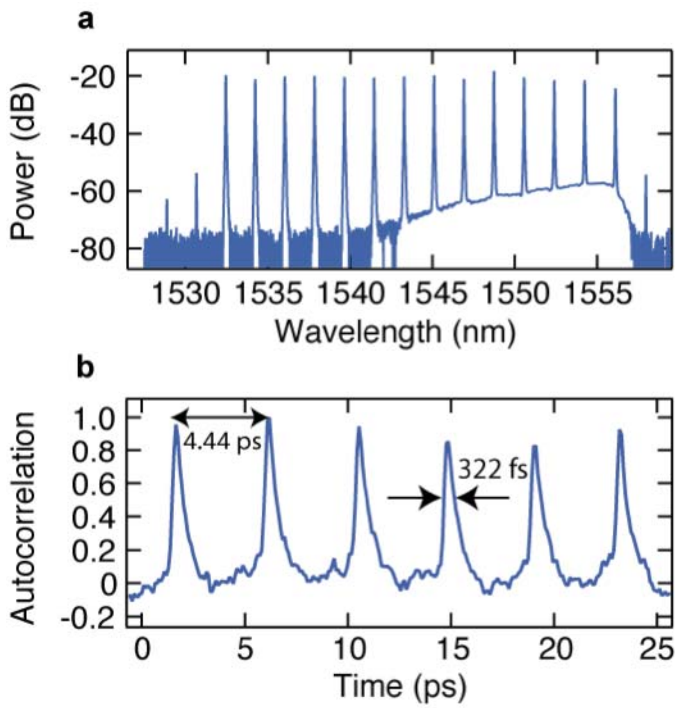

Figure 12. (a) Filtered optical spectrum of frequency comb with 225-GHz FSR. (b) Normalized autocorrelation trace of pulse train.

Finally, we investigate the pulse formation dynamics in a parametric comb. Similar to our previous measurements, we filter a 25-nm section of the comb. We split the filtered output and send it to an autocorrelator and an RF spectrum analyzer. We simultaneously monitor the autocorrelation trace of the pulses formed, the RF amplitude noise, and the unfiltered optical spectrum of the generated frequency comb. The results of the measurement are shown in Figure 13. The leftmost column shows the autocorrelation traces of generated temporal waveforms [Figure 13(a)], the middle column [Figure 13(b)] shows the RF noise spectrum and the rightmost column shows the optical spectrum of the generated frequency comb [Figure 13(c)] corresponding to each stage of pulse formation as the pump wavelength is tuned into resonance (top to bottom). The 25-nm filtered section of the frequency comb that is used for temporal characterization is represented in red color in each optical spectrum trace. As we tune into resonance and more power is coupled into the microresonator, small clusters of comb lines (mini-combs) begin to appear several free-spectral ranges away from the pump centered around the initially generated cascaded FWM peaks. Simultaneously, a train of pulses appears with pulse duration of ~700 fs and the several individual peaks are observed in the RF domain. As these mini-combs grow and the amplitude of the comb lines equalize, the pulse duration reduces. At the same time, however, the number of peaks in the RF domain increases and the linewidth of these peaks broadens. We attribute these peaks to beating between adjacent mini-combs due to the fact that, at this point in the comb formation process, the mini-combs are largely uncorrelated and each of these mini-combs have different comb spacings. As the comb lines equalize, more mini-combs begin to spectrally overlap, resulting in a significant increase in the RF noise. At the next stage, as we tune deeper into the resonance, the comb reaches a transition stage where the RF noise suddenly drops by >20 dB. We believe this is a result of phase-locking of the comb analogous to mode-locking in a femtosecond pulse source. The temporal waveform at this point is very sensitive to the energy of the individual comb lines being filtered and we observe modulations both in the autocorrelation and the optical spectrum. Finally, as the pump is tuned further into resonance, we again observe equalization of the amplitude of the comb lines, and pulses with the shortest duration are generated [30].

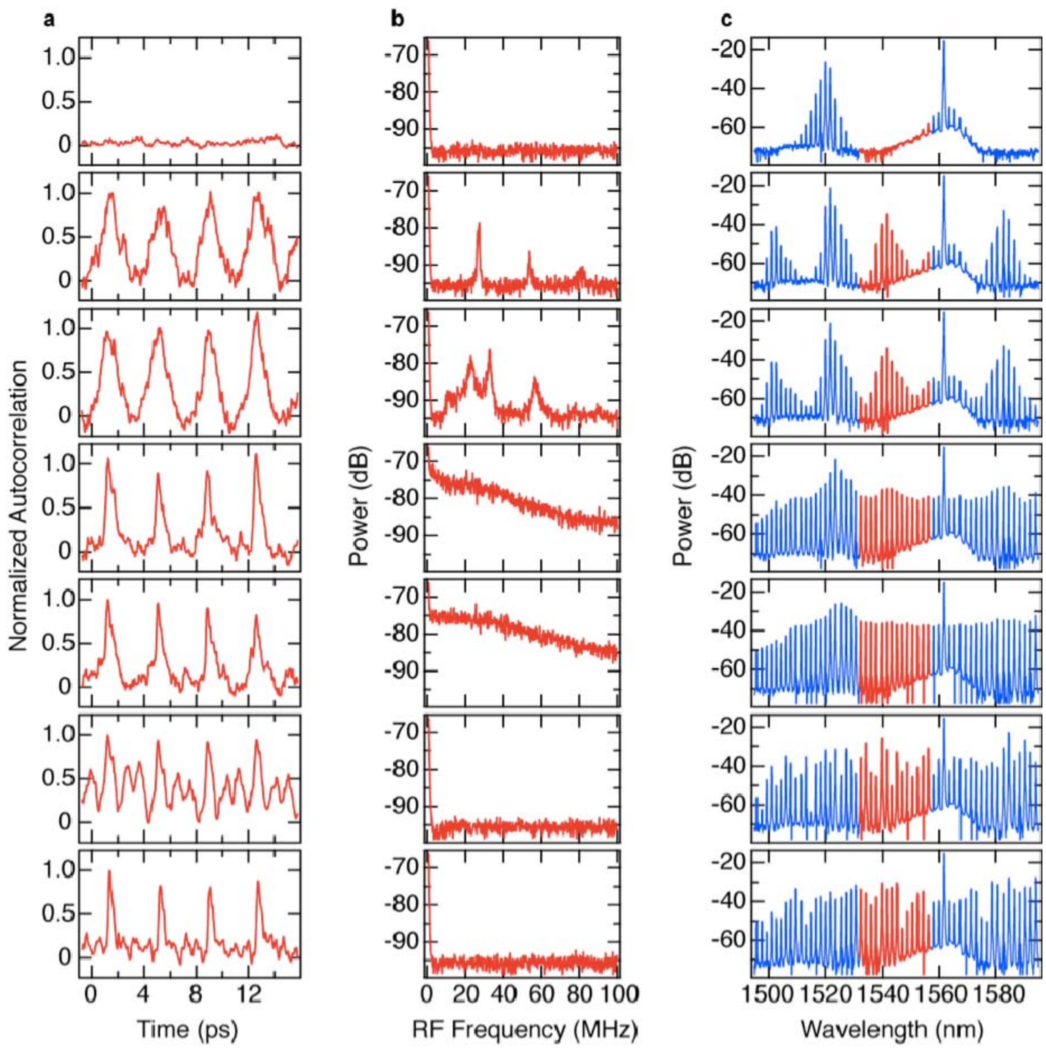

Figure 13. Comb generation dynamics. (a) Autocorrelation, (b) RF spectrum, and (c) optical spectrum as comb is generated.

8. Conclusions

We have developed the technology for parametric frequency comb generation in silicon nitride microresonators. Our platform allows for control over the operating wavelength and FSR, offering potential as a platform for comb generation over a wide wavelength spanning from visible to mid-IR with arbitrary comb spacing. In addition, due to the low-noise operation of the comb due to phase-locking behavior, the system offers potential, not only as a stabilized comb source for frequency domain applications, but also as a high-repetition rate ultrafast pulse source. As compared with femtosecond-laser-based frequency comb generation, parametric frequency comb generation is a technology that is not yet mature, and both theoretical and experimental studies are need to further understand the mechanisms governing the comb dynamics [29,31]. However, we believe our efforts are a significant step toward the development of an environmentally robust, ultra-compact, stabilized frequency comb source that can be used in applications such as spectroscopy, gas sensing, on-chip clock distribution for high-speed optical networks, remote clock synchronization, and photonic analog-to-digital conversion.

9. References

1. S. T. Cundiff and J. Ye, "Colloquium: Femtosecond optical frequency combs," Rev. Mod. Phys. 75, S. T 325 (2003).
2. J. Ye and S. T. Cundiff, *Femtosecond Optical Frequency Comb: Principle, Operation, and Applications* (Springer, New York, 2005).
3. M. J. Thorpe, K. D. Moll, J. J. Jones, B. Safdi, and J. Ye, "Broadband cavity ringdown spectroscopy for sensitive and rapid molecular detection," Science **311**, 1595-1599 (2006).
4. S. A. Diddams, L. Hollberg, V. Mbele, "Molecular fingerprinting with the resolved modes of a femtosecond laser frequency comb,"Nature **445**, 627-630 (2007).
5. D. J. Jones, S. A. Diddams, J. K. Ranka, A. Stentz, R. S. Windeler, J. L. Hall, and S. T. Cundiff, "Carrier-envelope phase control of femtosecond mode-locked lasers and direct optical frequency synthesis," Science **288**, 635-639 (2000).
6. R. Holzwarth, Th. Udem, T. W. Hänsch, J. C. Knight, W. J. Wadsworth, and P. St. J. Russell, "Optical frequency synthesizer for precision spectroscopy," Phys. Rev. Lett. **85**, 2264-2267 (2000).
7. Th. Udem, R. Holzwarth, and T. W. Hänsch, "Optical frequency metrology," Nature **416**, 233-237 (2002).
8. S. T. Cundiff, J. Ye, and J. L. Hall, "Optical frequency synthesis based on mode-locked lasers," Rev. Sci. Instrum. **72**, 3749 (2001).
9. R. Ell, U. Morgner, F. X. Kärtner, J. G. Fujimoto, E. P. Ippen, V. Scheuer, G. Angelow, T. Tschudi, M. J. Lederer, A. Boiko, and B. Luther-Davies, "Generation of 5-fs pulses and octave-spanning spectra directly from a Ti:sapphire laser," Opt. Lett. **26**, 373-375 (2001).
10. T. Fortier, A. Bartels, and S. A. Diddams, "Octave-spanning Ti:sapphire laser with a repetition rate >1 GHz for optical frequency measurements and comparisons," Opt. Lett. **31**, 1012-1014 (2006).
11. T. J. Kippenberg, R. Holzwarth, and S. A. Diddams, "Microresonator-based optical frequency combs," Nature **339**, 555-559 (2011).
12. P. Del'Haye, A. Schliesser, O. Arcizet, T. Wilken, R. Holzwarth, and T. J. Kippenberg, "Optical frequency comb generation from a monolithic microresonator," Nature **450**, 1214-1217 (2007).
13. I. H. Agha, Y. Okawachi, M. A. Foster, J. E. Sharping, and A. L. Gaeta, "Four-wave-mixing parametric oscillations in dispersion-compensated high-Q silica microspheres," Phys. Rev. A **76**, 043837 (2007).
14. A. A. Savchenkov, A. B. Matsko, V. S. Ilchenko, I. Solomatine, D. Seidel, and L. Maleki, "Tunable optical frequency comb with a crystalline whispering gallery mode resonator," Phys. Rev. Lett. **101**, 093902 (2008).
15. P. Del'Haye, O. Arcizet, A. Schliesser, R. Holzwarth, and T. J. Kippenberg, "Full stabilization of a microresonator frequency comb," Phys. Rev. Lett. **101**, 053903 (2008).
16. D. Braje, L. Hollberg, and S. Diddams, "Brillouin-enhanced hyperparametric generation of an optical frequency comb in a monolithic highly nonlinear fiber cavity pumped by a cw laser," Phys. Rev. Lett. **102**, 193902 (2009).
17. L. Razzari, D. Duchesne, M. Ferrera, R. Morandotti, S. Chu, B. E. Little, and D. J. Moss, "CMOS-compatible integrated optical hyperparametric oscillator," Nature Photonics **4**, 41-45 (2010).
18. P. Del'Haye, T. Herr, E. Gavartin, R. Holzwarth, and T. J. Kippenberg, "Octave spanning tunable frequency comb from a microresonator," Phys. Rev. Lett. **107**, 063901 (2011).
19. K. J. Vahala, "Optical microcavities," Opt Eng **424**, 839-846 (2003).

20. J. S. Levy, A. Gondarenko, M. A. Foster, A. C. Turner-Foster, A. L. Gaeta, and M. Lipson, "CMOS-compatible multiple-wavelength oscillator for on-chip optical interconnects," Nature Photonics **4**, 37-40 (2010).
21. M. A. Foster, J. S. Levy, O. Kuzucu, K. Saha, M. Lipson, and A. L. Gaeta, "Silicon-based monolithic optical frequency comb source," Opt. Express **19**, 14233-14239 (2011).
22. E. Dulkeith, F. Xia, L. Schares, W. M. Green, and Y. A. Vlasov, "Group index and group velocity dispersion in silicon-on-insulator photonic wires," Opt. Express **14**, 3853-3863 (2006).
23. A. C. Turner, C. Manolatou, B. S. Schmidt, M. Lipson, M. A. Foster, J. E. Sharping, and A. L. Gaeta, "Tailored anomalous group-velocity dispersion in silicon channel waveguides," Opt. Express **14**, 4357-4362 (2006).
24. D. T. H. Tan, K. Ikeda, P. C. Sun, and Y. Fainman, "Group velocity dispersion and self phase modulation in silicon nitride waveguides," Appl. Phys. Lett. **96**, 061101 (2010).
25. Y. Okawachi, K. Saha, J. S. Levy, Y. H. Wen, M. Lipson, and A. L. Gaeta, "Octave-spanning frequency comb generation in a silicon nitride chip," Opt. Lett. **36**, 3398-3400 (2011).
26. T. Carmon, L. Yang, and K. J. Vahala, "Dynamical thermal behavior and thermal self-stability of microcavities," Opt. Express **12**, 4742-4750 (2004).
27. Y. Okawachi, K. Saha, J. S. Levy, M. A. Foster, M. Lipson, and A. L. Gaeta, "Ultrabroadband frequency comb generation at 1 μm in a silicon nitride ring resonator," in CLEO:2011 - Laser Applications to Photonic Applications, OSA Technical Digest (CD) (Optical Society of America, 2011), paper CFK2.
28. A. R. Johnson, Y. Okawachi, J. S. Levy, J. Cardenas, K. Saha, M. Lipson, and A. L. Gaeta, "Chip-based frequency combs with sub-100-GHz repetition rates," Opt. Lett., doc. ID 159146 (posted 23 January 2012, in press).
29. T. Herr, J. Riemensberger, C. Wang, K. Hartinger, E. Gavartin, R. Holzwarth, M. L. Gorodetsky, and T. J. Kippenberg, "Universal dynamics of kerr frequency comb formation in microresonators," arXiv:1111.3071 (2011).
30. K. Saha, Y. Okawachi, B. Shim, J. S. Levy, M. A. Foster, M. Lipson, and A. L. Gaeta, "On-chip high-repetition-rate femtosecond source," in preparation (2012).
31. A. A. Savchenkov, A. B. Matsko, W. Liang, V. S. Ilchenko, D. Seidel, and L. Maleki, "Transient regime of Kerr frequnecy comb formation," arXiv:1111.3922 (2011).

List of Acronyms, Abbreviations, and Symbols

Acronym	Description
CMOS	complementary metal-oxide-semiconductor
EDFA	erbium-doped fiber amplifier
FSR	free spectral range
FWM	four-wave mixing
IR	infrared
OPO	optical parametric oscillator
OSA	optical spectrum analyzer
YDFA	ytterbium-doped fiber-amplifier